

Electronic theory for the normal-state spin dynamics in Sr_2RuO_4 : Anisotropy due to spin-orbit coupling

I. Eremin,^{1,2} D. Manske,¹ and K. H. Bennemann¹

¹*Institut für Theoretische Physik, Freie Universität Berlin, D-14195 Berlin, Germany*

²*Physics Department, Kazan State University, 420008 Kazan, Russia*

(Received 5 February 2002; published 23 May 2002)

Using a three-band Hubbard Hamiltonian we calculate within the random-phase approximation the spin susceptibility, $\chi(\mathbf{q}, \omega)$, and nuclear magnetic resonance spin-lattice relaxation rate, $1/T_1$, in the normal state of the triplet superconductor Sr_2RuO_4 and obtain quantitative agreement with experimental data. Most importantly, we find that due to spin-orbit coupling the out-of-plane component of the spin susceptibility χ^{zz} becomes at low temperatures two times larger than the in-plane one. As a consequence, strong incommensurate antiferromagnetic fluctuations of the quasi-one-dimensional xz and yz bands point into the z -direction. Our results provide further evidence for the importance of spin fluctuations for triplet superconductivity in Sr_2RuO_4 .

DOI: 10.1103/PhysRevB.65.220502

PACS number(s): 74.70.Pq, 74.20.Mn, 74.25.-q

The spin-triplet superconductivity with $T_c = 1.5$ K observed in layered Sr_2RuO_4 seems to be a new example of unconventional superconductivity.¹ The non- s -wave symmetry of the order parameter is observed in several experiments (see, for example, Refs. 2 and 3). Although the structure of Sr_2RuO_4 is the same as of the high- T_c superconductor $\text{La}_{2-x}\text{Sr}_x\text{CuO}_4$, its superconducting properties resemble those of superfluid ^3He . Most recently it was found that the superconducting order parameter is of p -wave type, but contains line nodes halfway between the RuO_2 planes.^{4,5} These results support Cooper pairing via spin fluctuations as one of the most probable mechanism to explain the triplet superconductivity in Sr_2RuO_4 . Therefore, theoretical and experimental investigations of the spin dynamics behavior in the normal and superconducting state of Sr_2RuO_4 are needed.

Recent studies by means of inelastic neutron scattering (INS) (Ref. 6) and nuclear magnetic resonance (NMR) (Ref. 7) of the spin dynamics in Sr_2RuO_4 reveal the presence of strong incommensurate fluctuations in the RuO_2 plane at the antiferromagnetic wave vector $\mathbf{Q}_i = (2\pi/3, 2\pi/3)$. As it was found in band-structure calculations,⁸ they result from the nesting properties of the quasi-one-dimensional d_{xz} and d_{yz} bands. The two-dimensional d_{xy} band contains only weak ferromagnetic fluctuations. The observation of the line nodes between the RuO_2 planes^{4,5} suggests strong spin fluctuations between the RuO_2 planes in z direction.⁹⁻¹¹ However, inelastic neutron scattering¹² observes that magnetic fluctuations are purely two-dimensional and originate from the RuO_2 plane. Both behaviors could result as a consequence of the magnetic anisotropy within the RuO_2 plane as indeed was observed in recent NMR experiments by Ishida *et al.*¹³ In particular, analyzing the temperature dependence of the nuclear spin-lattice relaxation rate on ^{17}O in the RuO_2 plane at low temperatures, they have demonstrated that the out-of-plane component of the spin susceptibility can become almost three times larger than the in-plane one. This strong and unexpected anisotropy disappears with increasing temperature.¹³

In this Rapid Communication we analyze the normal state spin dynamics of the Sr_2RuO_4 using the two-dimensional

three-band Hubbard Hamiltonian for the three bands crossing the Fermi level. We calculate the dynamical spin susceptibility $\chi(\mathbf{q}, \omega)$ within the random-phase approximation and show that the observed magnetic anisotropy in the RuO_2 plane arises mainly due to the spin-orbit coupling. Its further enhancement with lowering temperatures is due to the vicinity to a magnetic instability. Thus, we demonstrate that as in the superconducting state¹⁴ the spin-orbit coupling plays an important role also for the normal state spin dynamics of Sr_2RuO_4 . We also discuss briefly the consequences of this magnetic anisotropy for Cooper pairing due to the exchange of spin fluctuations.

We start from the two-dimensional three-band Hubbard Hamiltonian,

$$H = H_I + H_U = \sum_{\mathbf{k}, \sigma} \sum_l t_{\mathbf{k}l} a_{\mathbf{k}, l\sigma}^+ a_{\mathbf{k}, l\sigma} + \sum_{i,l} U_l n_{i\uparrow} n_{i\downarrow}, \quad (1)$$

where $a_{\mathbf{k}, l\sigma}$ is the Fourier-transformed annihilation operator for the d_l orbital electrons ($l = xy, yz, zx$) and U_l is the corresponding on-site Coulomb repulsion. $t_{\mathbf{k}l}$ denotes the energy dispersions of the tight-binding bands calculated as follows: $t_{\mathbf{k}l} = -\epsilon_0 - 2t_x \cos k_x - 2t_y \cos k_y + 4t' \cos k_x \cos k_y$. We choose the values for the parameter set $(\epsilon_0, t_x, t_y, t')$ as $(0.5, 0.42, 0.44, 0.14)$, $(0.24, 0.31, 0.045, 0.01)$, and $(0.24, 0.045, 0.35, 0.01)$ eV for d_{xy} , d_{zx} , and d_{yz} orbitals in accordance with band-structure calculations.¹⁵ The electronic properties of this model in application to Sr_2RuO_4 were studied recently and as was found can explain some features of the spin excitation spectrum in Sr_2RuO_4 .^{8,14,16,11} However, this model fails to explain the observed magnetic anisotropy at low temperatures¹³ and line nodes in the superconducting order parameter below T_c , which are between the RuO_2 planes. On the other hand, it is known that the spin-orbit coupling plays an important role in the superconducting state of in Sr_2RuO_4 .¹⁴ This is further confirmed by the recent observation of the large spin-orbit coupling in the insulating Ca_2RuO_4 .¹⁷ Therefore, we include in our model spin-orbit coupling,

$$H_{so} = \lambda \sum_i \mathbf{L}_i \mathbf{S}_i, \quad (2)$$

where the angular momentum \mathbf{L}_i operates on the three t_{2g} orbitals on the site i . Similar to an earlier approach,¹⁴ we restrict ourselves to the three orbitals, ignoring e_{2g} orbitals and choose the coupling constant λ such that the t_{2g} states behave like an $l=1$ angular momentum representation. Moreover, it is known that the quasi-two-dimensional xy band is separated from the quasi-one-dimensional xz and yz bands. Then, one expects that the effect of spin-orbit coupling is small and can be excluded for simplicity. Therefore, we consider the effect of the spin-orbit coupling on xz and yz bands only. Then, the kinetic part of the Hamiltonian $H_t + H_{so}$ can be diagonalized and the new energy dispersions are

$$\begin{aligned} \epsilon_{\mathbf{k},yz}^\sigma &= (t_{\mathbf{k},yz} + t_{\mathbf{k},xz} + A_{\mathbf{k}})/2, \\ \epsilon_{\mathbf{k},xz}^\sigma &= (t_{\mathbf{k},yz} + t_{\mathbf{k},xz} - A_{\mathbf{k}})/2, \end{aligned} \quad (3)$$

where $A_{\mathbf{k}} = \sqrt{(t_{\mathbf{k},yz} - t_{\mathbf{k},xz})^2 + \lambda^2}$, and σ refers to spin projection. One clearly sees that the spin-orbit coupling does not remove the Kramers degeneracy of the spins. Therefore, the resultant Fermi surface consists of three sheets like observed in the experiment. Most importantly, spin-orbit coupling together with Eq. (1) leads to a new quasiparticle that we label by pseudospin and pseudo-orbital indices. The unitary transformation $\tilde{U}_{\mathbf{k}}$ connecting old and new quasiparticles is defined for each wave vector and lead to the following relation between them:

$$\begin{aligned} c_{\mathbf{k},yz+}^+ &= u_{1\mathbf{k}} a_{\mathbf{k},yz+}^+ - i v_{1\mathbf{k}} a_{\mathbf{k},xz+}^+, \\ c_{\mathbf{k},xz+}^+ &= u_{2\mathbf{k}} a_{\mathbf{k},yz+}^+ - i v_{2\mathbf{k}} a_{\mathbf{k},xz+}^+, \\ c_{\mathbf{k},yz-}^+ &= u_{1\mathbf{k}} a_{\mathbf{k},yz-}^+ + i v_{1\mathbf{k}} a_{\mathbf{k},xz-}^+, \\ c_{\mathbf{k},xz-}^+ &= u_{2\mathbf{k}} a_{\mathbf{k},yz-}^+ + i v_{2\mathbf{k}} a_{\mathbf{k},xz-}^+, \end{aligned} \quad (4)$$

where $u_{m\mathbf{k}} = \lambda / \sqrt{(t_{\mathbf{k},yz} - t_{\mathbf{k},xz} \mp A_{\mathbf{k}})^2 + \lambda^2}$ and $v_{m\mathbf{k}} = (t_{\mathbf{k},yz} - t_{\mathbf{k},xz} \mp A_{\mathbf{k}}) / \sqrt{(t_{\mathbf{k},yz} - t_{\mathbf{k},xz} \mp A_{\mathbf{k}})^2 + \lambda^2}$. The “-” and “+” signs refer to the $m=1$ and $m=2$, respectively.

In Fig. 1 we show the resultant Fermi surfaces for each obtained band where we have chosen $\lambda = 100$ meV in agreement with earlier estimations.^{14,17} One immediately sees that xz and yz bands split around the nested parts in good agreement with experiment.¹⁸ Thus, spin-orbit coupling acts as a hybridization between these bands. However, in contrast to hybridization spin-orbit coupling introduces also an anisotropy for the states with pseudospins \uparrow and \downarrow . This will be reflected in the magnetic susceptibility. Since the spin and orbital degrees of freedom are now mixed in some spin-orbital liquid, the magnetic susceptibility involves also the orbital magnetism which is very anisotropic.

For the calculation of the transverse, χ_l^{+-} , and longitudinal, χ_l^{zz} , components of the spin susceptibility of each band l we use the diagrammatic representation. Since the Kramers degeneracy is not removed by the spin-orbit coupling, the

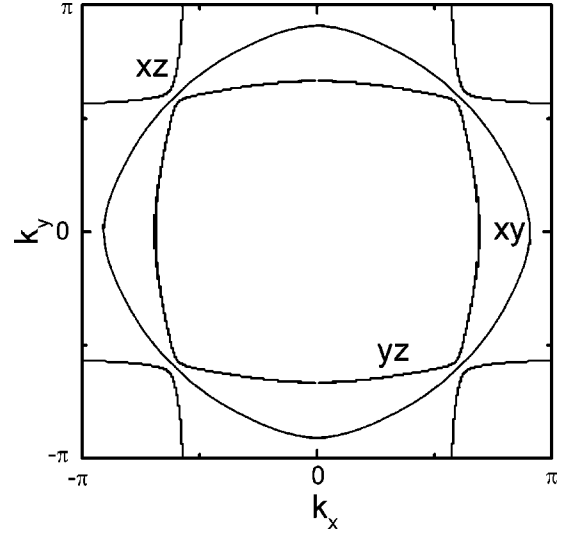


FIG. 1. Calculated Fermi surface for a RuO_2 plane in Sr_2RuO_4 taking into account spin-orbit coupling.

main anisotropy arises from the calculations of the anisotropic vertex $g_z = \tilde{l}_z + 2s_z$ and $g_+ = \tilde{l}_+ + 2s_+$ calculated on the basis of the new quasiparticle states. In addition, due to the hybridization between xz and yz bands we also calculate the transverse and longitudinal components of the inter-band susceptibility $\chi_{ll'}$. Then, for example,

$$\begin{aligned} \chi_{0,xz}^{+-}(\mathbf{q}, \omega) &= -\frac{4}{N} \sum_{\mathbf{k}} (u_{2\mathbf{k}} u_{2\mathbf{k}+\mathbf{q}} - v_{2\mathbf{k}} v_{2\mathbf{k}+\mathbf{q}})^2 \\ &\times \frac{f(\epsilon_{\mathbf{k}xz}^+) - f(\epsilon_{\mathbf{k}+\mathbf{q}xz}^-)}{\epsilon_{\mathbf{k}xz}^+ - \epsilon_{\mathbf{k}+\mathbf{q}xz}^- + \omega + iO^+}, \end{aligned} \quad (5)$$

and

$$\begin{aligned} \chi_{0,xz}^{zz}(\mathbf{q}, \omega) &= \chi_{xz}^\uparrow(\mathbf{q}, \omega) + \chi_{xz}^\downarrow(\mathbf{q}, \omega) \\ &= -\frac{2}{N} \sum_{\mathbf{k}} [u_{2\mathbf{k}} u_{2\mathbf{k}+\mathbf{q}} + v_{2\mathbf{k}} v_{2\mathbf{k}+\mathbf{q}} \\ &+ \sqrt{2}(u_{2\mathbf{k}} v_{2\mathbf{k}+\mathbf{q}} + v_{2\mathbf{k}} u_{2\mathbf{k}+\mathbf{q}})]^2 \\ &\times \frac{f(\epsilon_{\mathbf{k}xz}^+) - f(\epsilon_{\mathbf{k}+\mathbf{q}xz}^+)}{\epsilon_{\mathbf{k}xz}^+ - \epsilon_{\mathbf{k}+\mathbf{q}xz}^+ + \omega + iO^+}, \end{aligned} \quad (6)$$

where $f(x)$ is the Fermi function and $u_{\mathbf{k}}^2$ and $v_{\mathbf{k}}^2$ are the corresponding coherence factors that we have calculating through the corresponding vertexes using Eq. (4). For all other orbitals the calculations are straightforward. Note that the magnetic response of the xy band remains isotropic.

One clearly sees the difference between longitudinal and transverse components which results from the calculated matrix elements. Moreover, the longitudinal one gets an extra term due to \tilde{l}_z while the transverse does not contain the contributions from \tilde{l}_+ or \tilde{l}_- . The latter occurs due to the fact that xz and yz states are a combination of the real orbital states $|2, +1\rangle$ and $|2, -1\rangle$. Thus the transition between these

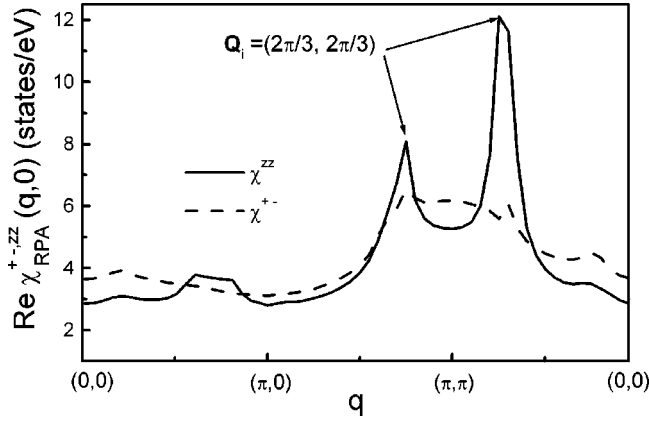


FIG. 2. Results for the real part of the out-of-plane (solid curve) and in-plane (dashed curve) magnetic susceptibilities, $\text{Re } \chi(\mathbf{q}, \omega)$, calculated within RPA using $U=0.505$ eV along the route $(0,0) \rightarrow (\pi,0) \rightarrow (\pi,\pi) \rightarrow (0,0)$ within the first Brillouin zone at temperature $T=100$ K.

two states are not possible with \tilde{T}_+ or \tilde{T}_- operators. Therefore, each component of the longitudinal susceptibility gets an extra term in the matrix element that sufficiently enhances their absolute values.

Assuming $U_{ij} = \delta_{ij}U$ one gets the following expressions for the transverse susceptibility within random-phase approximation (RPA):

$$\chi_{RPA,i}^{+-}(\mathbf{q}, \omega) = \frac{\chi_{0,i}^{+-}(\mathbf{q}, \omega)}{1 - U\chi_{0,i}^{+-}(\mathbf{q}, \omega)}, \quad (7)$$

and for the longitudinal susceptibility

$$\begin{aligned} \chi_{RPA,i}^{zz}(\mathbf{q}, \omega) \\ = \frac{\chi_{0,i}^{\uparrow}(\mathbf{q}, \omega) + \chi_{0,i}^{\downarrow}(\mathbf{q}, \omega) + 2U\chi_{0,i}^{\uparrow}(\mathbf{q}, \omega)\chi_{0,i}^{\downarrow}(\mathbf{q}, \omega)}{1 - U^2\chi_{0,i}^{\uparrow}(\mathbf{q}, \omega)\chi_{0,i}^{\downarrow}(\mathbf{q}, \omega)}. \end{aligned} \quad (8)$$

In Fig. 2 we show the results for the real part of the transverse and longitudinal total susceptibility, $\chi_{RPA,i}^{+-,zz} = \sum_i \chi_{RPA,i}^{+-,zz}$ along the route $(0,0) \rightarrow (\pi,0) \rightarrow (\pi,\pi) \rightarrow (0,0)$ in the first Brillouin zone for $U=0.505$ eV. Note the important difference between the two components. Most importantly, the incommensurate antiferromagnetic fluctuations (IAF) at $\mathbf{Q}_i = (2\pi/3, 2\pi/3)$ are present in the case of xz and yz bands *only* in the longitudinal components of the spin susceptibility, but not in the transverse ones. This is connected to the fact that the matrix elements type of $u_{\mathbf{k}}$ and $v_{\mathbf{k}}$ are important because they suppress transition between “+” and “-” bands for the transverse susceptibilities. The transverse susceptibility is larger than the longitudinal one at small values of \mathbf{q} indicating ferromagnetic fluctuations. These are mainly pointing in the RuO_2 plane. On the other hand, the longitudinal component shows a structure at the IAF wave vector indicating a direction of the IAF fluctuations perpendicular to the RuO_2 plane.

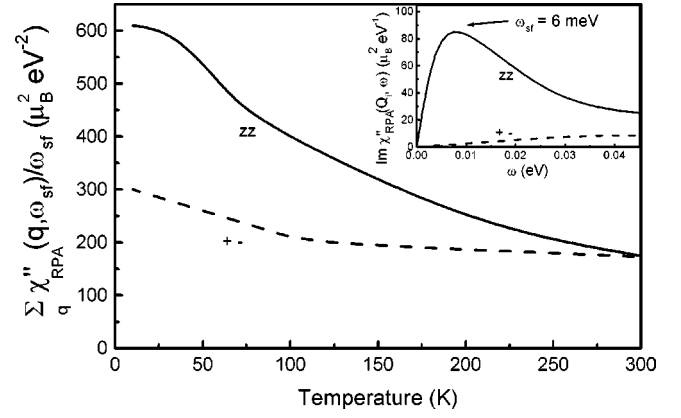


FIG. 3. Temperature dependence of the imaginary part of the spin susceptibility divided by ω_{sf} and summed over \mathbf{q} . Note, zz and $+-$ refer to the out-of-plane (solid curve) and in-plane (dashed curve) components of the RPA spin susceptibility. In the inset we show the corresponding frequency dependence of the $\text{Im } \chi_{RPA}(\mathbf{Q}_i, \omega)$ at the IAF wave vector $\mathbf{Q}_i = (2\pi/3, 2\pi/3)$. The results for the out-of-plane component (solid curve) are in a quantitative agreement with INS experiments (Ref. 6).

We also note that our results are in accordance with earlier estimations made by Ng and Sigrist¹⁹ with one important difference. In addition to Ng and Sigrist,¹⁹ we include in accordance with mixing of the spin and orbital degrees of freedom also the orbital contribution to the magnetic susceptibility χ . For example, due to l_z and l_{\pm} vertices at $\mathbf{Q}_i = (2\pi/3, 2\pi/3)$, χ^{zz} is affected by factor of 2 from spin-orbit coupling. Moreover, in previous work,¹⁹ it was found that the IAF are slightly enhanced in the longitudinal components of the xz and yz bands in comparison to the transverse one. In our case there are *no* IAF in the transverse component of the spin susceptibility. Furthermore, by taking into account the correlation effects within RPA we show that the IAF will be further enhanced in the z direction.

This is further illustrated in the inset of Fig. 3 where we present the results for the frequency dependence of the imaginary part of the total susceptibilities at $\mathbf{Q}_i = (2\pi/3, 2\pi/3)$ and temperature $T=20$ K. The longitudinal component reveals a peak at approximately $\omega_{sf} = 6$ meV in quantitative agreement with experimental data in INS.⁶ On the other hand, the transverse component is featureless showing the absence of the IAF spin fluctuations. This also points out that the IAF are aligned perpendicular to the RuO_2 plane.

In order to see the temperature dependence of the magnetic anisotropy induced by the spin-orbit coupling we display in Fig. 3 the temperature dependence of the quantity $\sum_{\mathbf{q}} \text{Im } \chi_{RPA}(\mathbf{q}, \omega_{sf}) / \omega_{sf}$ for both components. At room temperatures both longitudinal and transverse susceptibilities are almost identical, since thermal effects wash out the influence of the spin-orbit interaction. With decreasing temperature the magnetic anisotropy arises and at low temperatures we find the important result that the out-of-plane component χ^{zz} is about two times larger than the in-plane one ($\chi^{zz} > \chi^{+-}/2$).

Finally, in order to compare our results with experimental data we calculate the nuclear spin-lattice relaxation rate for

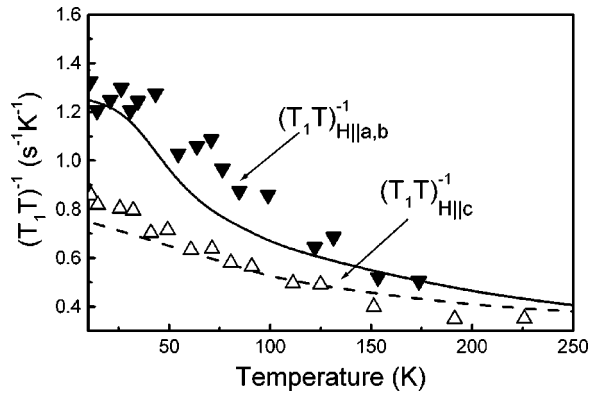


FIG. 4. Calculated normal-state temperature dependence of the nuclear spin-lattice relaxation rate T_1^{-1} of ^{17}O in the RuO_2 plane for the external magnetic field applied along c axis (dashed curve) and along the a - b plane (solid curve). Down and up triangles are experimental points taken from Ref. 13 for the corresponding magnetic-field direction.

^{17}O ion in the RuO_2 plane for different external magnetic field orientation ($i = a, b$, and c)

$$\left[\frac{1}{T_1 T} \right]_i = \frac{2k_B \gamma_n^2}{(\gamma_e \hbar)^2} \sum_{\mathbf{q}} |A_{\mathbf{q}}^p|^2 \frac{\chi_p''(\mathbf{q}, \omega_{sf})}{\omega_{sf}} \quad (9)$$

where $A_{\mathbf{q}}^p$ is the q -dependent hyperfine-coupling constant and χ_p'' is the imaginary part of the corresponding spin susceptibility, respectively, *perpendicular* to the i direction. Similar to experiment¹³ we use an isotropic hyperfine coupling constant ($^{17}\text{A}_{\mathbf{q}} \sim 22 \text{ kOe}/\mu_B$).

In Fig. 4 we show the calculated temperature dependence of the spin-lattice relaxation for an external magnetic field within and perpendicular to the RuO_2 plane together with experimental data. At $T = 250 \text{ K}$ the spin-lattice relaxation

rate is almost isotropic. Due to the anisotropy in the spin susceptibilities arising from spin-orbit coupling the relaxation rates become different with decreasing temperature. The largest anisotropy occurs close to the superconducting transition temperature in good agreement with experimental data.¹³

To summarize, our results clearly demonstrate the essential significance of spin-orbit coupling for the spin dynamics already in the normal state of the triplet superconductor Sr_2RuO_4 . We find that the magnetic response becomes strongly anisotropic even within a RuO_2 plane: while the in-plane response is mainly ferromagnetic, the out-of-plane response is antiferromagneticlike.

Let us also remark on the implication of our results for the triplet superconductivity in Sr_2RuO_4 . In a previous study,¹¹ neglecting spin-orbit coupling but including the hybridization between xy , xz , and yz bands, we have found ferromagnetic and IAF fluctuations within the a - b plane. This would lead to nodes within the RuO_2 plane. However, due to the magnetic anisotropy induced by spin-orbit coupling, a nodeless p -wave pairing is possible in the RuO_2 plane as experimentally observed. Our results provide further evidence for the importance of spin fluctuations for triplet superconductivity in Sr_2RuO_4 . Regarding the possibility of p -wave pairing within RuO_2 plane studied previously,^{20–22} note that the anisotropy considered in this paper might be significant for determining the position of the node in the RuO_2 plane or between two RuO_2 planes.

We are thankful to B.L. Gyorffy, Y. Maeno, K. Ishida, D. Fay, and M. Eremin for stimulating discussions and M.Ya. Ovchinnikova for a critical reading of the manuscript. We are grateful to INTAS (Work Program 654), SFB 290, and the German-French Foundation (PROCOPE) for financial support. The work of I. E. was supported by the ‘‘Alexander von Humboldt Foundation’’ and CRDF Grant No. REC. 007.

¹Y. Maeno *et al.*, Nature (London) **372**, 532 (1994).

²K. Ishida *et al.*, Phys. Rev. B **56**, R505 (1997).

³J.A. Duffy *et al.*, Phys. Rev. Lett. **85**, 5412 (2000).

⁴M.A. Tanatar, M. Suzuki, S. Nagai, Z.Q. Mao, Y. Maeno, and T. Ishiguro, Phys. Rev. Lett. **86**, 2649 (2001).

⁵K. Izawa, H. Takahashi, H. Yamaguchi, Y. Matsuda, M. Suzuki, T. Sasaki, T. Fukase, Y. Yoshida, R. Settai, and Y. Onuki, Phys. Rev. Lett. **86**, 2653 (2001).

⁶Y. Sidis *et al.*, Phys. Rev. Lett. **83**, 3320 (1999).

⁷H. Mukuda *et al.*, J. Phys. Soc. Jpn. **67**, 3945 (1998).

⁸I.I. Mazin and D.J. Singh, Phys. Rev. Lett. **82**, 4324 (1999).

⁹M.E. Zhitomirsky and T.M. Rice, Phys. Rev. Lett. **87**, 057001 (2001).

¹⁰J.F. Annett, G. Litak, B.L. Gyorffy, and K.I. Wysokinski, cond-mat/0109023 (unpublished).

¹¹I. Eremin, D. Manske, C. Joas, and K. H. Bennemann, Europhys. Lett. (to be published).

¹²F. Servant, S. Raymond, B. Fak, P. Lejay, and J. Flouquet, Solid State Commun. **116**, 489 (2000).

¹³K. Ishida, H. Mukuda, Y. Minami, Y. Kitaoka, Z.Q. Mao, H. Fukazawa, and Y. Maeno, Phys. Rev. B **64**, 100501(R) (2001).

¹⁴K.K. Ng and M. Sigrist, Europhys. Lett. **49**, 473 (2000).

¹⁵A. Liebsch and A. Lichtenstein, Phys. Rev. Lett. **84**, 1591 (2000).

¹⁶D.K. Morr, P.F. Trautman, and M.J. Graf, Phys. Rev. Lett. **86**, 5978 (2001).

¹⁷T. Mizokawa, L.H. Tjeng, G.A. Sawatzky, G. Ghiringhelli, O. Tjernberg, N.B. Brookes, H. Fukazawa, S. Nakatsuji, and Y. Maeno, Phys. Rev. Lett. **87**, 077202 (2001).

¹⁸A. Damascelli *et al.*, Phys. Rev. Lett. **85**, 5194 (2000).

¹⁹K.K. Ng and M. Sigrist, J. Phys. Soc. Jpn. **69**, 3764 (2000).

²⁰M. Sato and M. Kohmoto, J. Phys. Soc. Jpn. **69**, 3505 (2000).

²¹T. Kuwabara and M. Ogata, Phys. Rev. Lett. **85**, 4586 (2000).

²²K. Kuroki, M. Ogata, R. Arita, and H. Aoki, Phys. Rev. B **63**, 060506 (2001).